In addition, a fabrication scheme to realize millimeter-wave dielectric waveguide components is also described. This method offers a valid approach toward low cost millimeter-wave component and integrated circuit developments.

Acknowledgment

The authors would like to express their sincere appreciation to C. R. Ibscher and L. D. Thomas for technical assistance.

References

[1] J. Paul and Y. Chang, "Millimeter-wave image-guide integrated passive devices," *IEEE Trans. Microwave Theory Tech.*, vol. MTT-26, pp. 751–574, Oct. 1978.
[2] S. Shindo and T. Itanami, "Low-loss rectangular dielectric image line for millimeter-wave integrated circuits," *IEEE Trans. Microwave Theory Tech.*, vol. MTT-26, pp. 747–751, Oct. 1978.
[3] B. Song and T. Itoh, "A distributed feedback dielectric waveguide oscillator with a built-in leaky-wave antenna," *1979 IEEE MTT Int. Microwave Symp. Dig.*, (Orlando, FL), pp. 217–219, 1979.
[4] R. Mittra *et al.*, "Active integrated devices on dielectric substrates for millimeter-wave applications," *1979 IEEE MTT Int. Microwave Symp. Dig.*, (Orlando, FL), pp. 220–221, 1979.
[5] Products of Emerson & Cuming, Inc.
[6] W. Schlosser and H. Unger, "Partially filled waveguides and surface waveguides for rectangular cross section," in *Advances in Microwaves*, vol. 1, pp. 319–387, New York: Academic.
[7] E. Marcatili, "Dielectric rectangular waveguide and directional coupler for integrated optics," *Bell Syst. Tech. J.*, vol. 48, pp. 2071–1201, 1969.
[8] K. Solbach, "The calculation and the measurement of the coupling properties image lines of rectangular cross section," *IEEE Trans. Microwave Theory Tech.*, vol. MTT-27, pp. 54–58, Jan. 1979.
[9] C. Hoer, "Using six-port and eight-port junctions to measure active and passive circuit parameters," NBS Tech. Note 673, Sept. 1975.
[10] G. F. Engen, "An improved circuit for implementing the six-port technique of microwave measurements," *IEEE Trans. Microwave Theory Tech.*, vol. MTT-26, pp. 1080–1083, Dec. 1977.

Jeffrey A. Paul (S'73–M'75) was born in Long Beach, CA, in 1952, and received the B.S.E.E. degree at Carnegie-Mellon University in 1974 and the M.S.E.E. degree at Stanford University, in Stanford, CA, in 1976. He began working at the Missile Systems Division of Hughes Aircraft Company in 1974 as a Hughes Fellow in the area of airborne radar systems. In 1975 he joined the Electron Dynamics Division, working on millimeter-wave integrated circuits. He is currently Assistant Manager of the Microwave Circuits Department and is involved in research and development of millimeter-wave mixers, radar sensors, and integrated components.

Percy C. H. Yen was born in Shanghai, China, in 1942, and received the B.S. degree from Cheng Kung University, Tainan, Taiwan, and the Ph.D. degree from the University of Pennsylvania, Philadelphia, both in electrical engineering, in 1964 and 1968, respectively. From 1969 to 1973, he had Post-Doctoral positions at Columbia, Rockefeller, and Columbia Universities with primary interest area in RF systems and instrumentation.

His first industrial position was at Bunker-Ramo Corporation, Westlake, CA, where he was engaged in the development of parametric amplifiers and ferrite devices. Later he was employed by Transco Products, Inc., Venice, CA, working on switches and coplanar antennas and by TRW, Redondo Beach, CA, working on RF transmitter and receiver design. In 1978, he worked at Ford Aerospace and Communication Corporation, Newport Beach, CA, working on the design of IMPATT oscillators and combiners. Since June 1979, he has been with Electron Dynamics Division, Hughes Aircraft Company, Torrance, CA, and involved in developing mixers, VCO's, dielectric guide components and integrated circuit, all in the millimeter-wave region.

Millimeter-Wave Dielectric Image Line Detector-Circuit Employing Etched Slot Structure

KLAUS SOLBACH

Abstract—**In an earlier paper [1] slots in the ground plane are investigated as new circuit elements in dielectric image lines. In this paper slots in dielectric image lines employing metallized dielectric substrates as the ground plane are investigated. It is shown that this configuration can be used to realize truly integrated dielectric image line semiconductor circuits. As an example the design and performance of a detector circuit for 26 to 40 GHz is presented.**

Manuscript received November 24, 1980; revised March 26, 1981. This work was supported by the German Research Society (DFG) under Contract Wo 137/6.

The author was with University Duisburg, Duisburg, Germany. He is now with AEG-Telefunken, 7900 Ulm, Germany.

I. Introduction

IN AN EARLIER paper slots in the ground plane of the dielectric image line were proposed as mode launchers and circuit elements [1]. It is shown that the slot discon-

0018-9480/81/0900-0953$00.75 ©1981 IEEE

tinuity can be described as a junction of the dielectric waveguide and a metal waveguide (groove) extending from the slot into the ground plane. In the plane of the slot, fields are excited, which radiate into the space above the junction. Due to the dielectric layer above the slot this radiation can be effectively shielded, depending on the permittivity and the thickness of the dielectric.

In this paper slot discontinuities in dielectric image lines employing metallized dielectric substrates as the ground plane are investigated. The major advantage over slot discontinuity elements in solid metal ground planes is that this configuration lends itself to photo-etching techniques of production.

In the analysis of the structure the method presented in [1] is adapted to yield an approximate equivalent circuit of the discontinuity. The results of the analysis are used in the design of a practical detector circuit.

II. The Slot Structure

The slot discontinuity structure is shown in Fig. 1. The upper metallization layer of a dielectric substrate acts as the image plane of the dielectric image line. The slot in the metallization layer acts as a transverse discontinuity in the dielectric image line.

A T-equivalent circuit consisting of two series impedances Z_s and one parallel impedance may be used to describe the slot. Since only narrow slots are of interest here the parallel impedance may be neglected. The series impedances can be determined by inserting an electric wall in the symmetry plane of the slot. Following the method of analysis employed in [1] the slot approximately is modelled as a discontinuity in a planar electric wall resonator, Fig. 2, that means the finite width of the dielectric image line and the slot is neglected. In the Appendix the complete set of potentials is given to describe the fields in each subregion of the resonator structure. It is obvious that in region I and region IV propagating waves may exist (in z-direction and in y-direction, respectively), which represent radiation into the space above the slot and into the dielectric substrate.

Subsequently the fields in each subregion are matched along the boundaries to yield the eigenvalue equation of the disturbed resonator in the same manner as described in [1].

From the eigenfrequency of the resonator the slot series impedance Z_s is calculated using (1) in [1]. In the following discussion the metallization thickness was neglected ($t=0$).

In Fig. 3. the calculated impedance components (a parallel-circuit configuration of R_s and X_s assumed) are plotted versus the normalized thickness of the dielectric substrate. The slot reactance dependence for small substrate thickness is similar to that of the slot reactance in the solid ground plane case described in [1], but it is different above cutoff of the first higher order mode E_1 in the substrate. The real component R_s behaves totally different to that in the solid ground plane case, expressing the leakage of power into the substrate: R_s is zero for vanishing substrate thickness and approaches the radiation resistance of the slot in a solid ground plane ($R_s/Z_{L2}=3$). Above the cutoff of the first higher mode in the substrate the slot resistance sharply decreases since additional power is lost in the E_1 mode.

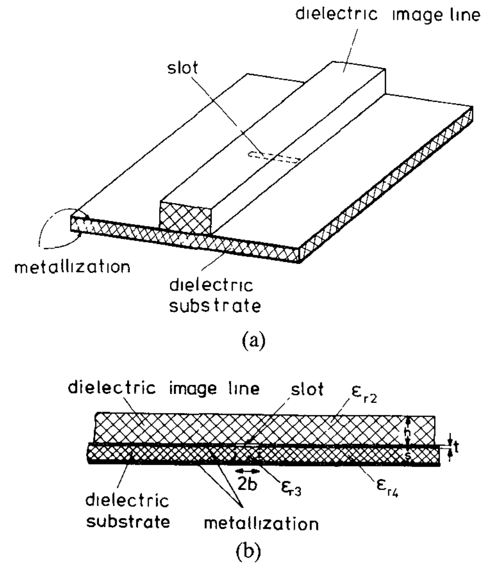

Fig. 1. A slot in the ground plane of a dielectric image line employing a metallized substrate as the ground plane.

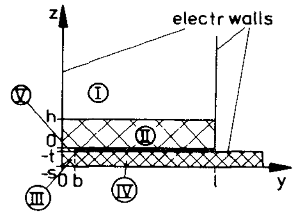

Fig. 2. Planar resonator model for a slot in the metallization of a dielectric substrate.

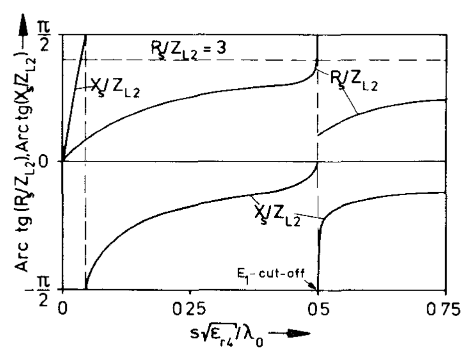

Fig. 3. The normalized slot resistance and slot reactance calculated as a function of the normalized substrate thickness (Z_{L2} = characteristic impedance of dielectric image line, region II) $\epsilon_{r2}=5$, $\epsilon_{r3}=\epsilon_{r4}=2$, $4h\sqrt{\epsilon_{r2}-1}/\lambda_0=1.2$, $2b/\lambda_2=0.1$.

Analyses of this relationship have led to the equivalent circuit representation shown in Fig. 4, valid only in the fundamental mode region of the substrate ($s\sqrt{\epsilon_{r4}}/\lambda_0<0.5$). The slot impedance is represented by the radiation resistance R_s, describing the radiation loss above the dielectric image line, and a capacitor C_s, describing the electrical fringe fields of the slot. Additionally, two waveguides are connected in parallel, one short-circuited waveguide, describing the standing wave-like field distribution between the slot and the lower metallization plane of the dielectric substrate, and one waveguide, matched with its own char-

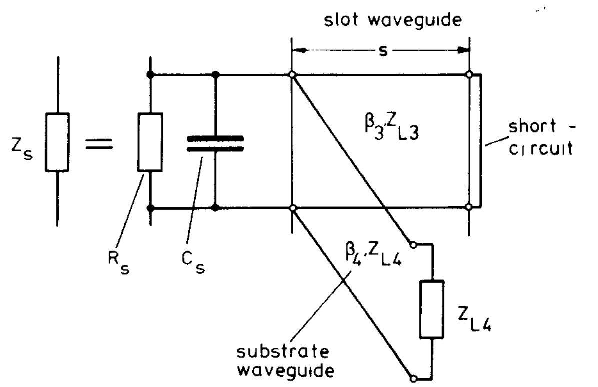

Fig. 4. Approximate equivalent circuit representation for a slot in the metallization of a dielectric substrate. (Z_{L3}, Z_{L4} = characteristic impedances, and β_3, β_4 = phase constants in regions III and IV, respectively).

acteristic impedance $Z_{L4}=(Z_0 s)/(\sqrt{\epsilon_{r4}})$, to describe the loading of the slot due to the wave launched in the substrate.

It is interesting to note that the power loss due to the radiation into the substrate is proportional to the characteristic admittance $1/Z_{L4}$ of the substrate waveguide. That means, in order to achieve low radiation losses in the substrate a low permittivity substrate of relatively large thickness must be used.

The losses due to the radiation into the space above the dielectric image line can be considered to be the same as in the solid ground plane case: Due to the interference effects of waves traveling directly from the slot and waves from reflections at the dielectric–air interface $z=h$ and at the image plane $z=0$, these losses decrease with increasing permittivity of the dielectric waveguide and exhibit a minimum for a normalized height $h\sqrt{\epsilon_{r2}}/\lambda_0 \approx 0.4$ of the dielectric guide [1].

III. Detector-Circuit

Several methods are known from the literature for the implementation of semiconductor devices in millimeter-wave dielectric waveguides.

Kuno and Chang [2] as well as Jacobs and Chrepta [3] have reported open, unshielded circuits employing metal strips on top of the dielectric guide (similar to microstripline) to couple the semiconductor devices to the dielectric waveguide. Some radiation loses in these circuits are hardly avoidable. Wiltse [4] described a coaxial detector diode with the inner conductor protruding from the ground plane into the dielectric image line. A parabolic reflector is used to focus the incident wave to the diode and to reduce radiation losses.

On the other hand several circuits have been reported (e.g. [5], [6]) employing modified metal waveguide mounts with horn-launcher section to couple to the dielectric waveguide. Though this approach may yield best results with respect to the availability of design data and to the efficiency of the circuits it is not truely amendable for integration into dielectric image line circuits.

Aylward and Williams [5] as well as Paul and Chang [7] as a compromise between open, unshielded circuits and metal waveguide circuits, present circuits where the dielectric guide surface is metallized to enclose the integrated semiconductor devices. This technique successfully eliminates radiation losses from the semiconductor devices but heavy radiation losses occur at the transition from the open dielectric guide to the metallized dielectric guide.

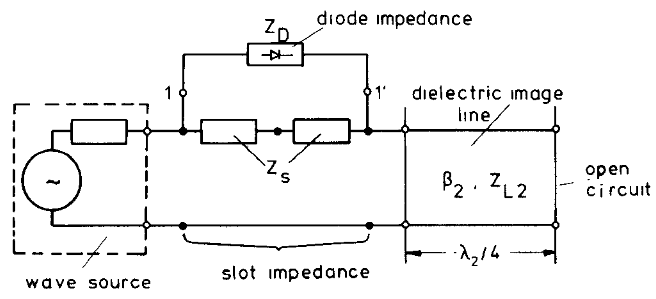

Fig. 5. Equivalent circuit representation of a detector circuit using a slot in the metallization of a dielectric substrate.

TABLE I
The Optimum Achievable Delaunching Efficiency for a Slot in a Metallized Substrate

ϵ_{r2}	η
12	-0.67 dB
5	-1.63 dB
2.22	-3.54 dB

It is now straight foreward to utilize the described slot structure as a basis for detector and mixer circuits. The fundamental principle of operation is 1) that a slot in the dielectric image line can provide a two-terminal source to a mixer- or detector-diode, and 2) that the guide above the slot can act as a dielectric shielding to reduce radiation losses in the circuit.

The equivalent circuit representation of a detector circuit using a slot in the dielectric image line is given in Fig. 5. The waveguide is open circuited at a quarter-wavelength distance from the slot to bring the slot into a position, where the current across the slot is a maximum. The diode impedance Z_D is shown to be connected across the slot, in parallel to the full slot impedance $2Z_s$.

The incident wave on the dielectric image line is delaunched into the diode if Z_D is matched to the source impedance at terminals $1-1'$. The delaunching efficiency

$$\eta=\frac{1}{1+1/(2R_s/Z_{L2})} \tag{1}$$

is readily calculated for the equivalent circuit Fig. 5 and, using numerical results for the slot series impedance, in Table I the optimum values of the delaunching efficiency are listed for three different values of the dielectric constant ϵ_{r2}. For these calculations the permittivity and thickness of the dielectric substrate were chosen $\epsilon_{r3}=\epsilon_{r4}=2$ and $s\sqrt{\epsilon_{r4}}/\lambda_0=0.25$.

From Table I it can be seen that only a high permittivity dielectric image line may be employed to achieve a high efficiency detector circuit.

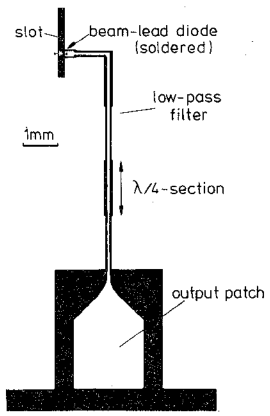

Fig. 6. Layout for the photolithographic production of the metallization pattern of the detector circuit for 26 to 40 GHz. White: metal; black: etched away.

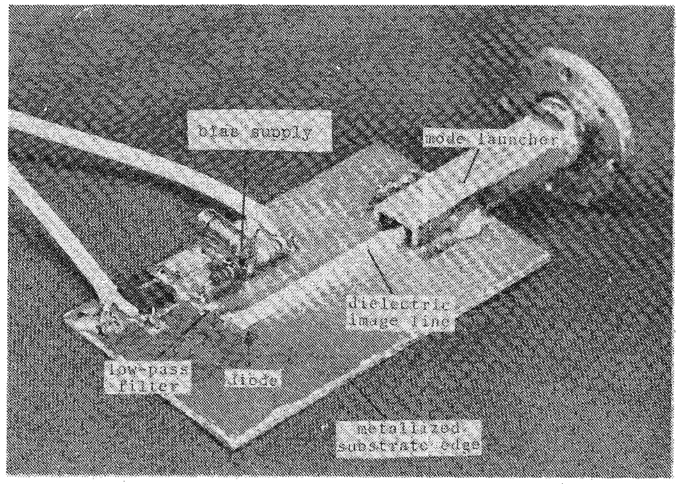

Fig. 7. Photograph of the completed detector module.

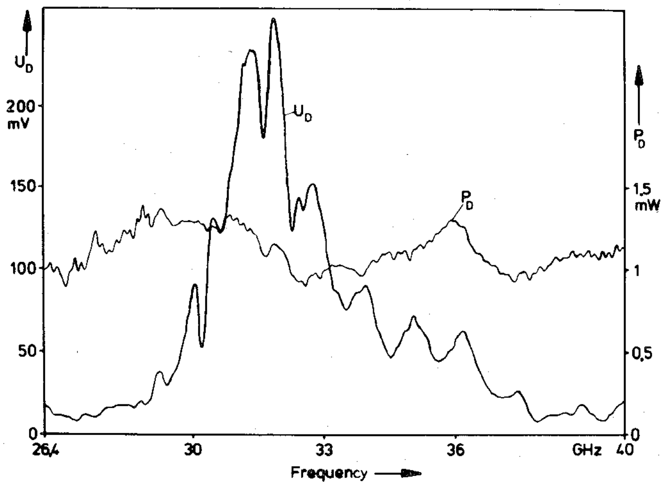

Fig. 8. Incident power P_D and output voltage U_D measured for the detector module as a function of the frequency.

A practical detector-circuit was designed for the frequency range 26–40 GHz. The metallization pattern shown in Fig. 6 was etched on a copper plated RT/Duroid 5880 substrate ($\epsilon_{r4} = 2.2$).

The slot was designed as a half-wavelength resonant slot for midband so that the low impedance beam-lead diode (DMK-6606, Alpha Industries) could be tap-matched to the high source impedance presented across the slot.

The dielectric image guide was cut from an Epsilam-10[1] substrate ($\epsilon_r = 10$). The guide was equipped with a slight groove where the slot structure is covered in order not to break the beam-lead diode when the guide was fixed to the substrate. The slight air-gap between the guide and the image plane can be neglected since the normal electric field strength at this location is zero (current maximum). The guide is truncated at about a quarter-wavelength distance from the slot (open-circuit).

The height $h = 1.25$ mm of the guide was chosen near the optimum value of $h\sqrt{\epsilon_{r2}}/\lambda_0 = 0.4$. The width of the guide $2w = 2.5$ mm was chosen to maintain fundamental mode operation of the dielectric image line. The dielectric substrate thickness $s = 1.58$ mm was chosen near the optimum value of $s\sqrt{\epsilon_{r4}}/\lambda_0 = 0.25$.

The dc current from the diode is carried to an output patch via a coplanar low-pass filter also etched in the substrate metallization layer. Since the diode used exhibits a pronounced threshold-characteristic (mixer diode), in the detector application described here, it was necessary to apply a bias current of about 0.1 mA to achieve highest sensitivity.

The complete detector module is shown in Fig. 7. The dielectric image line is excited through a metal waveguide mode launcher consisting of a truncated metal waveguide releasing the tip of the dielectric guide. The circuitry for the supply of the dc bias can be seen on one side. The RF blocking properties of the dc line are enhanced by the use of two small pieces of dielectric fixed to the low-impedance sections of the low-pass filter.

In spite of this an appreciable amount of RF field was detected in the bias supply area on the substrate and along the edges of the substrate. This clearly is due to radiation from the slot into the substrate, which cannot be suppressed totally in the present design. To reduce the radiation losses, the edges of the substrate were metallized by applying conducting-silver paint.

The measured detector output voltage for an incident power level of about 1 mW is plotted in Fig. 8 as a function of the frequency. For this measurement the open-circuit termination of the dielectric image line behind the slot was adjusted to optimize the circuit performance at about 32 GHz. It can be seen that the sensitivity of the module is about 250 mV/mW around 32 GHz, including the losses in the mode launcher (≈ 1 dB), the dielectric image line section (≈ 1 dB) and in the open-circuit termination. This figure compares quite well with the performance of commercially available tunable metal waveguide detector circuits.

IV. Conclusion

It has been shown that the realization of a detector-circuit using a slot in the ground plane of a dielectric image line is feasible. The described technique offers a way to a true integration of semiconductor devices into dielectric image

[1]3M Company.

line millimeter-wave circuits. Although not presented in this paper, the described slot structures have also been used to realize traveling wave slot antennas and periodic structure bandstop filters.

Appendix
The Resonator Eigenvalue Equation

The fields of the resonator of Fig. 2 are derived from E^y-potentials to describe the fundamental TM-mode characteristics of the slot discontinuity. The series expansion of the potential functions in the five regions of the resonator are

$$\begin{aligned}
\Pi^{\mathrm{I}} &= \sum_{k=0}^{\infty} F_k \cos\left(\frac{k\pi}{1} y\right) e^{-\gamma_k z} \\
\Pi^{\mathrm{II}} &= \sum_{k=0}^{\infty} \cos\left(\frac{k\pi}{1} y\right)\left[B_k \cos(\beta_{zk} z) + B_k' \sin(\beta_{zk} z)\right] \\
\Pi^{\mathrm{III}} &= \sum_{n=0}^{\infty} \sin(\beta_{yn} y)\Big[H_n \cos\Big(\frac{n\pi}{s}(z+s)\Big) \\
&\quad + H_n' \sin\Big(\frac{n\pi}{s}(z+s)\Big)\Big] \\
\Pi^{\mathrm{IV}} &= \sum_{\mu=0}^{\infty} G_\mu e^{-j\beta_{y\mu}} \cos\left(\frac{\mu\pi}{s} z\right) \\
\Pi^{\mathrm{V}} &= \sum_{\nu=0}^{\infty} \cos\left(\frac{\nu\pi}{b} y\right)\left[F_\nu \sin(\beta_{z\nu} z) + F_\nu' \cos(\beta_{z\nu} z)\right]
\end{aligned} \tag{A.1}$$

with

$$\begin{aligned}
k_0^2 &= \left(\frac{k\pi}{1}\right)^2 - \gamma_k^2 \\
k_0^2 \epsilon_{r2} &= \left(\frac{k\pi}{1}\right)^2 - \beta_z^2 k \\
k_0^2 \epsilon_{r3} &= \left(\frac{n\pi}{s}\right)^2 + \beta_{yn}^2 \\
k_0^2 \epsilon_{r4} &= \left(\frac{\mu\pi}{s}\right)^2 + \beta_{y\mu}^2 \\
k_0^2 &= \left(\frac{\nu\pi}{b}\right)^2 + \beta_{z\nu}^2
\end{aligned} \tag{A.2}$$

and $k_0 = (2\pi)/(\lambda_0) = (2\pi/C_0)f =$ wavenumber of free space.

The E_y- and the transversal H_x- and E_z-field strengths can be derived from the given potentials using well-known methods, e.g., [8].

The amplitude coefficients have to be chosen so that the continuity conditions for the tangential fields are satisfied along the subregions boundaries. For the plane $z=h$ this leads to the eigenvalue equation of the TM-modes on the dielectric slab guide (matrix-formulation, see [1])

$$\overleftrightarrow{S} \cdot \vec{B} + \overleftrightarrow{S}' \cdot \vec{B}' = 0 \tag{A.3}$$

where $\overleftrightarrow{S}$ and $\overleftrightarrow{S}'$ are diagonal matrices containing the resonance conditions for even and odd TM-modes. The formulation of the continuity condition for the plane $z=0$ is also identical to the case described in [1]

$$\vec{B} = \overleftrightarrow{R} \cdot \vec{F}' \tag{A.4}$$

and

$$\vec{F}' = \overleftrightarrow{Q} \cdot \vec{B}'. \tag{A.5}$$

The mode matching along planes $z=-t$ and $y=b$ is performed in the same manner yielding

$$\vec{F}' = \overleftrightarrow{P} \cdot \vec{H}' \tag{A.6}$$

$$\vec{F} = \overleftrightarrow{T} \cdot \vec{H} \tag{A.7}$$

$$\vec{H} = \overleftrightarrow{W} \cdot \vec{H}'. \tag{A.8}$$

By suitable combination of equations (A.4) through (A.8) the coupling of the even and odd TM-modes on the dielectric image line resonator can be described by

$$\begin{aligned}
\vec{B} &= \overleftrightarrow{R} \cdot \overleftrightarrow{P} \cdot \overleftrightarrow{W}^{-1} \cdot \overleftrightarrow{T}^{-1} \cdot \overleftrightarrow{Q} \cdot \vec{B}' \\
&= \overleftrightarrow{V} \cdot \vec{B}'
\end{aligned} \tag{A.9}$$

so that the resonator eigenvalue equation takes the form of

$$(\overleftrightarrow{S} \cdot \overleftrightarrow{V} + \overleftrightarrow{S}') \cdot \vec{B}' = 0. \tag{A.10}$$

The eigenvalue equation (A.10) can be solved for the resonance frequency in the usual manner by suitably truncating the matrices and searching for the zero of the system determinant.

References

[1] K. Solbach, "Slots in dielectric image line as mode launchers and circuit elements," *IEEE Trans. Microwave Theory Tech.*, vol. MTT-29, pp. 10–16, Jan. 1981.

[2] H. J. Kuno and Y. Chang, "Millimeter-wave integrated circuits," U.S. Army Electronics Command, Rep. No. ECOM-73-0297-F, May 1974.

[3] H. Jacobs, G. Novick, C. M. LoCascio, and M. Chrepta, "Measurement of guide wavelength in rectangular dielectric waveguide," *IEEE Trans. Microwave Theory Tech.*, vol. MTT-24, pp. 815–820, Nov. 1976.

[4] J. C. Wiltse, "Some characteristics of dielectric image lines at millimeter wavelengths," *IRE Trans. Microwave Theory Tech.*, vol. MTT-7, pp. 60–65, Jan. 1959.

[5] M. J. Aylward and N. Williams, "Feasibility studies of insular guide millimeterwave integrate circuits," in *Proc. AGARD Conf. Millimeter and Submillimeter Wave Propagation and Circuits* (München, Germany), Sept. 4–8, 1978 (Conference Reprint No. 245, pp. 30-1–30-11).

[6] B. J. Levin and J. E. Kietzer, "Hybrid millimeter-wave integrated circuits," U.S. Army Electronics Command, Final Rep. ECOM-74-0577-F, Oct. 1975.

[7] J. A. Paul and Yu-Wen Chang, "Millimeter-wave image-guide integrated passive devices," *IEEE Trans. Microwave Theory Tech.*, vol. MTT-26, pp. 751–754, Oct. 1978.

[8] R. F. Harrington, *Time-Harmonic Electromagnetic Fields.* New York: McGraw-Hill, 1961.

Klaus Solbach was born in Witten, Germany in 1951. He received the Dipl. -Ing. degree from the Technical University of Aachen,/ Aachen, Germany in 1974 and the Dr. -Ing. degree from the University Duisburg, Duisburg, Germany, in 1979.

From 1975 to 1979 he has been employed at the University Duisburg as a Research Assistant. He has been engaged in investigations of the properties and circuit applications of dielectric image lines in the millimeter wave frequency range. In 1980 he joined AEG-Telefunken, Ulm, Germany, as a Millimeterwave R&D Engineer.